

# Heteroclinic switching between chimeras

Christian Bick

*Oxford Centre for Industrial and Applied Mathematics,*

*Mathematical Institute, University of Oxford, OX2 6GG, UK*

*Centre for Systems Dynamics and Control and Department of Mathematics,*

*University of Exeter, EX4 4QF, UK*

(Dated: March 10, 2017)

## Abstract

Functional oscillator networks, such as neuronal networks in the brain, exhibit switching between metastable states involving many oscillators. Chimeras—localized frequency synchrony patterns—are candidates for such states, but their spatial location has predominantly been considered fixed. We show that dynamical transitions of the location of frequency synchrony arise in paradigmatic phase oscillator networks through metastable chimeras joined by heteroclinic connections. We illuminate the mechanisms that underly switching between chimeras in these experimentally accessible networks.

PACS numbers: 05.45.Xt, 05.65.+b

Sequential activity patterns involving metastable states have long been thought to be involved in neural computation [1, 2]. They arise on a microscopic scale where activity switches between individual neurons [3] as well as on a macroscopic scale where the metastable states involve the activity of many neurons [4]. Sequential activity through “winnerless competition” has also been hypothesized to play a role in cognitive function, often modeled by Lotka–Volterra type equations [5–8] that discard individual oscillator dynamics. On the level of individual units, however, information in neural networks is related to spatially localized dynamics (examples range from place cells [9] and gradient sensitive cells [10] to persistent activity in neural field models [11, 12]). Thus, chimeras—oscillatory patterns characterized by spatially localized frequency synchrony—are candidates to play a functional role in neural dynamics [13–15]. While chimeras have received much attention recently [16, 17] (also in neural networks [18, 19]), their spatial location has mostly been considered as static [20]. Is it possible to observe sequential switching dynamics between chimeras that yield dynamical transitions of the spatial location of frequency synchrony?

In this article we illuminate how weak chimeras together with connecting heteroclinic orbits arise in small phase oscillator networks. As weak chimeras [21–23] are characterized in terms of frequency synchrony along trajectories, the network dynamics will exhibit dynamical transitions between different patterns of localized frequency synchrony. Heteroclinic connections between weak chimeras are facilitated by network coupling which involves non-pairwise interaction terms depending on three or more phases [24, 25]. Such terms are not present in the classical Kuramoto model [26] but arise naturally in the phase reduction of more general oscillators [27]. Here, the nonpairwise coupling induces additional symmetries that make the system analytically tractable. In contrast to heteroclinics dynamics studied in networks of coupled neurons [28, 29], the saddle invariant sets of interest here are characterized by the collective dynamics of multiple oscillators. More precisely, trajectories on the saddle invariant sets will have two or more oscillators that are not frequency synchronized. Such dynamics cannot occur in phase oscillator networks with full permutational symmetry where one observes sequential switching between different phase locking patterns; see also [2, Section 7]. Our results elucidate the mechanisms that give rise to dynamical transitions of localized frequency synchrony—dynamics that bridge the levels of individual oscillators (synchrony) and collective dynamics (switching)—in networks that are accessible to experimental realization [30].

In the following, we consider networks of  $M$  populations of  $N$  phase oscillators. Let  $\theta_{\sigma,k} \in \mathbf{T} := \mathbb{R}/2\pi\mathbb{Z}$  denote the phase of oscillator  $k$  in population  $\sigma$ . Write  $\theta = (\theta_1, \dots, \theta_M) \in \mathbf{T}^{MN}$  where  $\theta_\sigma = (\theta_{\sigma,1}, \dots, \theta_{\sigma,N}) \in \mathbf{T}^N$  is the state of population  $\sigma$ . The set  $\mathbf{S} := \{(\phi_1, \dots, \phi_N) \in \mathbf{T}^N \mid \phi_k = \phi_{k+1}\}$  corresponds to phase synchrony and  $\mathbf{D} := \{(\phi_1, \dots, \phi_N) \in \mathbf{T}^N \mid \phi_{k+1} = \phi_k + \frac{2\pi}{N}\}$  denotes the splay phase where phases are distributed uniformly on the circle. Following [31] we use the shorthand notation

$$\theta_1 \cdots \theta_{\sigma-1} \mathbf{S} \theta_{\sigma+1} \cdots \theta_M = \{\theta \in \mathbf{T}^{MN} \mid \theta_\sigma \in \mathbf{S}\} \quad (1a)$$

$$\theta_1 \cdots \theta_{\sigma-1} \mathbf{D} \theta_{\sigma+1} \cdots \theta_M = \{\theta \in \mathbf{T}^{MN} \mid \theta_\sigma \in \mathbf{D}\} \quad (1b)$$

to indicate that population  $\sigma$  is phase synchronized or in splay phase. Hence,  $\mathbf{S} \cdots \mathbf{S}$  ( $M$  times) is the set of cluster states and  $\mathbf{D} \cdots \mathbf{D}$  is the set where all populations are in splay phase. Given a dynamical system on  $\mathbf{T}^{MN}$  and a trajectory  $\theta(t)$  with initial condition  $\theta(0) = \theta^0$ , define the asymptotic average angular frequency  $\Omega_{\sigma,k}(\theta^0) := \lim_{T \rightarrow \infty} \frac{1}{T} \theta_{\sigma,k}(T)$ . Recall that the characterizing feature of a *weak chimera* as a particular invariant set  $A \subset \mathbf{T}^{MN}$  is *frequency synchrony* (and lack thereof): for all  $\theta^0 \in A$  we have oscillators  $(\sigma, k)$ ,  $(\tau, j)$ ,  $(\rho, \ell)$  such that  $\Omega_{\sigma,k}(\theta^0) = \Omega_{\tau,j}(\theta^0) \neq \Omega_{\rho,\ell}(\theta^0)$ ; see [21–23] for a precise definition.

*Heteroclinic cycles in small networks*—Consider a network of  $M = 3$  populations of  $N = 2$  oscillators where the dynamics of population  $\sigma \in \{1, 2, 3\}$  is given by

$$\dot{\theta}_{\sigma,1} = g(\theta_{\sigma,2} - \theta_{\sigma,1}) - \varepsilon \text{snp}(\theta_{\sigma,2}, \theta_{\sigma,1}; \theta_{\sigma-1}) + \varepsilon \text{snp}(\theta_{\sigma,2}, \theta_{\sigma,1}; \theta_{\sigma+1}) =: X_{\sigma,1}(\theta), \quad (2a)$$

$$\dot{\theta}_{\sigma,2} = g(\theta_{\sigma,1} - \theta_{\sigma,2}) - \varepsilon \text{snp}(\theta_{\sigma,1}, \theta_{\sigma,2}; \theta_{\sigma-1}) + \varepsilon \text{snp}(\theta_{\sigma,1}, \theta_{\sigma,2}; \theta_{\sigma+1}) =: X_{\sigma,2}(\theta), \quad (2b)$$

and indices are taken modulo  $M$ . Here, interaction between oscillators within populations is pairwise and determined by

$$g(\vartheta) = \sin(\vartheta + \alpha) + r \sin(2(\vartheta + \alpha)) \quad (3)$$

while oscillators in different populations interact through the sinusoidal **non**pairwise interaction function

$$\text{snp}(\phi, \vartheta; \theta_\tau) = \cos(\theta_{\tau,1} - \theta_{\tau,2} + \phi - \vartheta + \alpha) + \cos(\theta_{\tau,2} - \theta_{\tau,1} + \phi - \vartheta + \alpha) \quad (4)$$

involving differences of four phases;  $\alpha, r \in \mathbb{R}$  are parameters. The coupling induces symmetries: (2) is  $(\mathbf{S}_N \times \mathbf{T})^N \rtimes \mathbb{Z}_M$ -equivariant. For each population,  $\mathbf{T}$  acts by shifting all

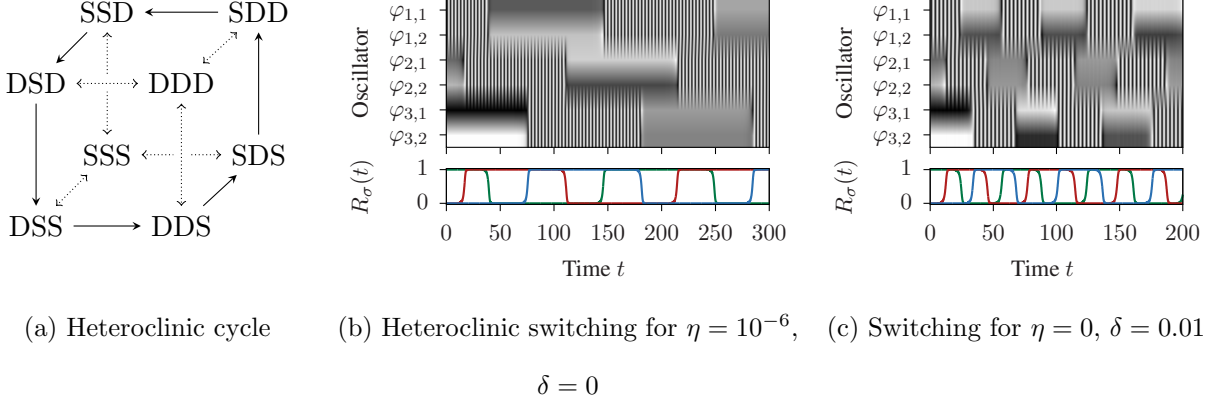


Figure 1. Heteroclinic networks appear in networks of  $M = 3$  populations of  $N = 2$  oscillators (5) with coupling function (3) where  $\alpha = \frac{\pi}{2}$ ,  $r = -0.1$ ,  $\varepsilon = 0.1$ . Panel (a) shows the heteroclinic cycle between saddle weak chimeras (solid lines); stability is indicated by arrows. Panel (b) shows noise induced switching close to the heteroclinic cycle: the phase evolution of each oscillator—shading indicates the phase from  $\theta_{\sigma,k} = \pi$  (black) to  $\theta_{\sigma,k} = 0$  (white)—and the order parameters  $R_\sigma$  (colors) are plotted over time. The phase evolution clearly shows transient frequency synchrony between different populations. Panel (c) shows switching dynamics for  $\delta > 0$  when the system only has a global phase shift symmetry. The initial condition is  $\theta^0 = (1, 1.1, 2, 5.14, 3.2, 0)$  in both (b) and (c).

phases of that population by a common constant while the symmetric group  $\mathbf{S}_N$  permutes the  $N$  oscillators of the population, and  $\mathbb{Z}_M := \mathbb{Z}/M\mathbb{Z}$  permutes populations cyclically. The semidirect product “ $\rtimes$ ” indicates that actions do not necessarily commute [32]. The symmetries induce invariant subspaces [33]: in particular SSS, DDD as well as DSS, DDS and their images under permutations of populations are dynamically invariant.

We can now give conditions for (2) to have the heteroclinic cycle depicted in Figure 1(a) between saddle weak chimeras DSS, DDS and their symmetric counterparts. Because of symmetry it suffices to show that the invariant sets DSS, DDS are (i) weak chimeras of (ii) saddle type which (iii) are connected by heteroclinic orbits. In the following, we focus on the case  $\alpha = \frac{\pi}{2}$  and refer to [34] for more generality and a proof that there is in fact an open set of parameters  $(\alpha, \varepsilon, r)$  for which this heteroclinic cycle between weak chimeras exists.

For DSS, DDS to be weak chimeras, (i), we calculate the frequencies  $\Omega_{\sigma,k}$  in (2). For  $\varepsilon = 0$  we have  $\Omega_{1,k}(\theta^0) = g(0) = 1$  for  $\theta^0 \in S\theta_2\theta_3$  and  $\Omega_{2,k}(\theta^0) = g(\pi) = -1$  for  $\theta^0 \in \theta_1 D\theta_3$ . For  $\varepsilon \geq 0$  and coupling (3), this implies  $\Omega_{1,k}(\theta^0) \neq \Omega_{2,k}(\theta^0)$  for  $\theta^0 \in SD\theta_3$  if  $|1 - (-1)| - 4\varepsilon > 0$ . At the same time,  $\Omega_{\sigma,k}(\theta^0) = \Omega_{\sigma,j}(\theta^0)$  for all  $\theta^0 \in \mathbf{T}^{MN}$  with  $\theta_\sigma^0 \in S, D$ . As a result DSS,

DDS are weak chimeras for (2) on  $\mathbf{T}^{MN}$  if  $2\varepsilon < 1$ .

For DSS, DDS to be saddle invariant sets, (ii), we reduce the phase-shift symmetries by rewriting (2) in terms of phase differences  $\psi_{\sigma,k} := \theta_{\sigma,k+1} - \theta_{\sigma,1}$ ,  $k = 1, \dots, N-1$ . (Consequently, we may replace all  $\theta$  by the phase differences  $\psi$  in (1).) Since  $N = 2$  here,  $\psi_\sigma = \psi_{\sigma,1}$  determines the state of population  $\sigma$  and the effective dynamics of (2) are three-dimensional. In the reduced system the sets DSS =  $(\pi, 0, 0)$ , DDS =  $(\pi, \pi, 0)$  are equilibria. Linearizing at DSS yields eigenvalues  $\lambda_1^{\text{DSS}} = 4r$ ,  $\lambda_2^{\text{DSS}} = 8\varepsilon + 4r$ ,  $\lambda_3^{\text{DSS}} = -8\varepsilon + 4r$  that correspond to linear stability of the first, second, and third population, respectively. Similarly, for DDS we obtain the eigenvalues  $\lambda_1^{\text{DDS}} = 8\varepsilon + 4r$ ,  $\lambda_2^{\text{DDS}} = -8\varepsilon + 4r$ ,  $\lambda_3^{\text{DDS}} = 4r$ . Observe that if  $0 < -r < 2\varepsilon$  we have  $\lambda_1^{\text{DSS}} = \lambda_3^{\text{DDS}} < 0$ ,  $\lambda_2^{\text{DSS}} = \lambda_1^{\text{DDS}} > 0$ ,  $\lambda_3^{\text{DSS}} = \lambda_2^{\text{DDS}} < 0$  and thus DSS, DDS are saddle invariant sets with two-dimensional stable and one-dimensional unstable manifold.

Finally, for the stability of DSS, DDS above, we obtain conditions for heteroclinic connections between the saddles, (iii). Observe that  $\lambda_2^{\text{DSS}} > 0$ ,  $\lambda_2^{\text{DDS}} < 0$  implies that the unstable manifold of DSS and the stable manifold of DDS both intersect the invariant subspace  $D\psi_2S$  on which the dynamics reduce to  $\dot{\psi}_2 = \sin(\psi_2)(8\varepsilon - 4r \cos(\psi_2))$ . Thus, if  $-r < 2\varepsilon$  there are no equilibria other than  $\psi_2 \in \{0, \pi\}$  (these are DSS and DDS) in  $D\psi_2S$  and we have a heteroclinic connection. Indeed, we get the same condition for there to be no additional equilibria in  $\psi_1DS$ . To summarize, for  $\alpha = \frac{\pi}{2}$  the heteroclinic cycle sketched in Figure 1(a) exists if  $0 < -r < 2\varepsilon < 1$  [35].

The heteroclinic cycle yields switching dynamics between the saddle weak chimeras which persist when the particular symmetries (and invariant subspaces) of (2) are broken. We integrated the system

$$\dot{\theta}_{\sigma,k} = X_{\sigma,k}(\theta) + \delta S_{\sigma,k}(\theta) + \eta W_{\sigma,k} \quad (5)$$

numerically in XPP [36] with  $X_{\sigma,k}$  as in (2), independent Wiener processes  $W_{\sigma,k}$ , and a symmetry breaking coupling term  $S_{\sigma,k}(\theta) = \frac{1}{MN} \sum_{(\tau,j)} \sin(\theta_{\tau,j} - \theta_{\sigma,k})$ . For  $\eta > 0$ ,  $\delta = 0$  we obtain heteroclinic switching where the time spent close to a saddle weak chimera scales with the noise amplitude  $\eta$ ; cf. Figure 1(b). Setting  $\delta > 0$  breaks the  $N$  phase-shift symmetries and reduces them to a single phase-shift symmetry which acts as a common phase shift to all oscillators. Interestingly, we still obtain switching dynamics prescribed by the heteroclinic network as shown in Figure 1(c).

*Order parameter dependent coupling induces switching*—The dynamical mechanism which

leads to heteroclinic cycles in (2) can be best understood if the oscillator network is seen as individual populations coupled through their mean fields. Let  $i = \sqrt{-1}$ . The absolute value of the Kuramoto order parameter  $R_\sigma := R(\theta_\sigma) = \left| \frac{1}{N} \sum_{j=1}^N \exp(i\theta_{\sigma,j}) \right|$  gives information about synchronization:  $\theta_\sigma \in S$  iff  $R(\theta_\sigma) = 1$  and  $\theta_\sigma \in D$  implies  $R(\theta_\sigma) = 0$ . Now consider a system of  $M$  populations of  $N$  phase oscillators each where the dynamics of oscillator  $k$  in population  $\sigma$  are given by

$$\dot{\theta}_{\sigma,k} = \frac{1}{N} \sum_{j \neq k} g(\theta_{\sigma,j} - \theta_{\sigma,k} + \Delta\alpha_\sigma) \quad (6)$$

with coupling function

$$g(\vartheta) = \sin(\vartheta + \alpha) + r \sin(n(\vartheta + \alpha)) \quad (7)$$

where  $n \in \mathbb{N}$ . If  $r = 0$  then either full synchrony  $S$  or the splay phase  $D$  is the global attractor for the dynamics (6) depending on the value of  $\alpha + \Delta\alpha_\sigma$  [37]. In particular, the global attractors swap stability at  $\alpha + \Delta\alpha_\sigma = \pm \frac{\pi}{2}$ . Now set

$$\Delta\alpha_\sigma = \varepsilon((1 - R_{\sigma-1}^2) - (1 - R_{\sigma+1}^2)) \quad (8)$$

for  $0 \leq \varepsilon \ll \frac{\pi}{2}$ . This dependency on the order parameters yields a mechanism for switching of synchrony if  $\alpha = \frac{\pi}{2}$  and  $r = 0$ : if population  $\sigma - 1$  is synchronized ( $R_{\sigma-1} = 1$ ) and population  $\sigma + 1$  is in splay phase ( $R_{\sigma+1} = 0$ ) then  $S$  is asymptotically stable for population  $\sigma$ . Conversely, if  $R_{\sigma+1} = 1$  and  $R_{\sigma-1} = 0$  then  $D$  is asymptotically stable for population  $\sigma$ . While the system is degenerate for  $R_{\sigma-1} = R_{\sigma+1}$  if  $\alpha = \frac{\pi}{2}$  and  $r = 0$ , an appropriate choice of  $n$  and  $r \neq 0$  can resolve this degeneracy by inducing bistability of  $S$  and  $D$ .

Nonpairwise coupling yields an approximation of the state-dependent phase shift (8) in (6). With (8) we obtain

$$g(\vartheta + \Delta\alpha_\sigma) = g(\vartheta) + \varepsilon(R_{\sigma+1}^2 - R_{\sigma-1}^2) \cos(\vartheta + \alpha) + O(\varepsilon^2) + O(\varepsilon r). \quad (9)$$

Generalizing (4), define the **sinusoidal nonpairwise scaled** interaction function

$$\text{snps}(\phi, \vartheta; \theta_\tau) = \frac{1}{N^2} \sum_{p,q=1}^N \cos(\theta_{\tau,p} - \theta_{\tau,q} + \phi - \vartheta + \alpha).$$

Note that  $R_\tau^2 = \frac{1}{N^2} \sum_{p,q=1}^N \cos(\theta_{\tau,p} - \theta_{\tau,q})$  which implies

$$R_\tau^2 \cos(\theta_{\sigma,j} - \theta_{\sigma,k} + \alpha) = \text{snps}(\theta_{\sigma,j}, \theta_{\sigma,k}; \theta_\tau). \quad (10)$$

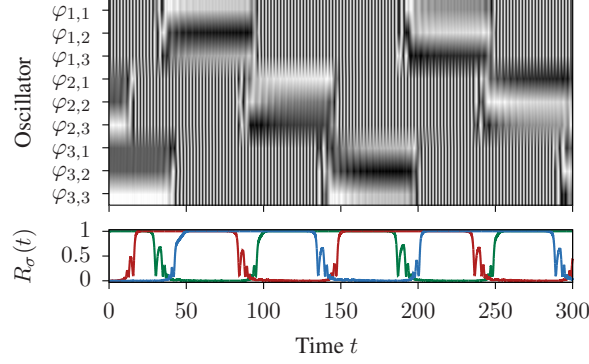


Figure 2. Switching between localized frequency synchrony is observed in networks of  $M = 3$  populations of  $N = 3$  oscillators with dynamics (5) and vector field (11). As in Figure 1 we plot the evolution of phases and order parameters over time. Coupling is given by (7) with  $q = 6$ ,  $r = -0.01$ ,  $\alpha = \frac{\pi}{2}$  and we have parameters  $\delta = 0.01$ ,  $\varepsilon = 0.2$ ,  $\eta = 10^{-5}$ . The initial conditions is  $\theta^0 = (1, 1.05, 1.1, 2, 4.1, 6.1, 2.1, 4.25, 0)$ .

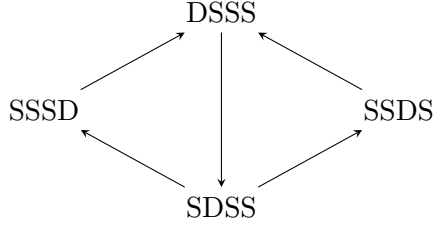
Substituting (9) and (10) into (6) and dropping the  $O(\varepsilon^2)$ ,  $O(\varepsilon r)$  terms now yields the phase dynamics

$$\dot{\theta}_{\sigma,k} = \frac{1}{N} \sum_{j \neq k} \left( g(\theta_{\sigma,j} - \theta_{\sigma,k}) - \varepsilon \text{snps}(\theta_{\sigma,j}, \theta_{\sigma,k}; \theta_{\sigma-1}) + \varepsilon \text{snps}(\theta_{\sigma,j}, \theta_{\sigma,k}; \theta_{\sigma+1}) \right) =: X_{\sigma,k}(\theta) \quad (11)$$

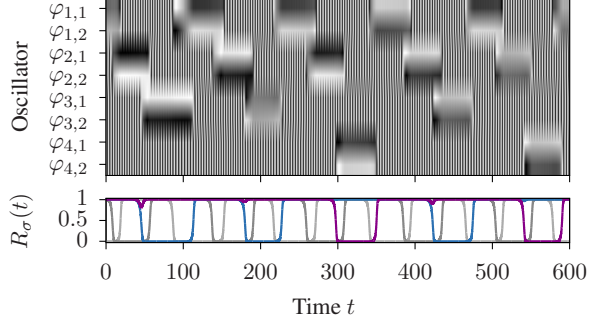
as an approximation of (6). Note that the system (2) with coupling function (3) above is—up to rescaling of  $\varepsilon$ —exactly this approximation for  $M = 3$ ,  $N = 2$ , and coupling (7) with harmonic  $n = 2$ .

*Switching dynamics for larger networks*—The derivation of the nonpairwise coupling suggests a general mechanism to obtain switching dynamics in systems with population sizes  $N > 2$  if there is a coupling function that yields bistability between full synchrony and the splay phase. For  $N = 3$  oscillators the coupling function (7) with  $n = 6$  induces bistability between S and D around  $\alpha = \frac{\pi}{2}$  for an uncoupled population. Integrating (5) with this particular coupling function for  $M = 3$ ,  $N = 3$ , and  $X_{\sigma,k}$  as in (11) yields switching dynamics even with a nontrivial symmetry breaking term  $\delta > 0$ ; cf. Figure 2. Note that any saddle connection now lies in a two-dimensional invariant subspace.

*From heteroclinic cycles to networks*—Generalizing the order parameter-dependent coupling (8) for the dynamics (6) leads to switching similar to those observed for the Kirk–Silber heteroclinic network [38] which contains more than one cycle; cf. Figure 3(a). Consider



(a) A Kirk-Silber type network between weak chimeras



(b) Temporal evolution of the phase oscillator network

Figure 3. The network of  $M = 4$  populations of  $N = 2$  oscillators with dynamics (12) shows noise induced random switching from SDSS to either SSDS or SSSD. This relates to the Kirk-Silber type network sketched in Panel (a). Panel (b) depicts evolution of phases and order parameters (populations 3 and 4 are highlighted in color) for coupling (3) with  $r = -0.1$ ,  $\alpha = 1.56$ , parameters  $\delta = 0.01$ ,  $\varepsilon = 0.35$ ,  $\eta = 10^{-4}$  and initial condition  $\theta^0 = (2, 5.14, 1, 1.1, 0.1, 0, 0.1, 0)$ .

$M = 4$  populations of  $N = 2$  oscillators with dynamics

$$\dot{\theta}_{1,k} = g(\theta_{1,3-k} - \theta_{1,k} - \varepsilon(1 - R_2^2) + \varepsilon(1 - R_3^2) + \varepsilon(1 - R_4^2)) + \delta S_{1,k}(\theta) + \eta W_{1,k} \quad (12a)$$

$$\dot{\theta}_{2,k} = g(\theta_{2,3-k} - \theta_{2,k} + \varepsilon(1 - R_1^2) - \varepsilon(1 - R_3^2) - \varepsilon(1 - R_4^2)) + \delta S_{2,k}(\theta) + \eta W_{2,k} \quad (12b)$$

$$\dot{\theta}_{3,k} = g(\theta_{3,3-k} - \theta_{3,k} - \varepsilon(1 - R_1^2) + \varepsilon(1 - R_2^2) - \varepsilon(1 - R_4^2)) + \delta S_{3,k}(\theta) + \eta W_{3,k} \quad (12c)$$

$$\dot{\theta}_{4,k} = g(\theta_{4,3-k} - \theta_{4,k} - \varepsilon(1 - R_1^2) + \varepsilon(1 - R_2^2) - \varepsilon(1 - R_3^2)) + \delta S_{4,k}(\theta) + \eta W_{4,k} \quad (12d)$$

with coupling function  $g$  as in (3). In contrast to (8), the  $\Delta\alpha_\sigma$  in (6) are now chosen to allow for switching from SDSS to either SSDS or SSSD. Figure 3(b) shows noise induced switching in (12) even with a nontrivial symmetry breaking term,  $\delta > 0$ . A full analysis of this system (and its nonpairwise approximation) is beyond the scope of this article.

*Discussion*—Phase oscillator networks with nonpairwise coupling have surprisingly rich dynamics [24, 25, 27]; here, nonpairwise interaction allows to show the existence of heteroclinic connections between weak chimeras. The main motivation for our nonpairwise coupling was a bifurcation parameter that depends on *local* order parameters of different populations. By contrast, the dynamics of a network with a bifurcation parameter depending on the *global* order parameter has been studied in their own right [39] and exploited for applications [40]. While sequential switching of phase synchrony has been observed before



for nonidentical oscillators [41], the system here consists of indistinguishable phase oscillators (the symmetry action is transitive) close to bifurcation. That is, small perturbations to the vector field are sufficient to go from one switching behavior to another.

Our results open up a range of questions relating both chimeras and heteroclinic networks. Are there heteroclinic cycles between saddle weak chimeras with chaotic dynamics [22]? Is it possible to realize any heteroclinic network in a phase oscillator network where the saddles are weak chimeras, see also [42, 43]? How do the dynamics of (12) relate to results obtained for the Kirk–Silber network [44]?

Heteroclinic switching between localized frequency synchrony patterns is of direct relevance for real-world systems. On the one hand, note that the small networks considered here are accessible for experimental realizations: weak chimeras have recently been engineered in electrochemical systems [30] by using feedback to realize desired network interactions [45]. Thus, we are interested in whether switching of localized frequency synchrony is observed in these experimental setups. On the other hand, sequential switching of localized frequency synchrony may be an important aspect of functional dynamics in networks of neurons. Our results elucidate the features of network interaction (e.g., symmetries, nonpairwise interactions) and the dynamical mechanisms that facilitate switching dynamics. Thus, our insights may open up ways to restore and control functional dynamics, for example, if the network becomes pathologically synchronized.

*Acknowledgements*—The author would like to thank M. Field, E. A. Martens, O. Omel’chenko, T. Pereira, M. Rabinovich, M. Wolfrum, and in particular P. Ashwin for many helpful discussions. This work has received funding from the People Programme (Marie Curie Actions) of the European Union’s Seventh Framework Programme (FP7/2007–2013) under REA grant agreement no. 626111.

- 
- [1] P. Ashwin and M. Timme, *Nature* **436**, 36 (2005).
  - [2] P. Ashwin, S. Coombes, and R. Nicks, *J Math Neurosci* **6**, 2 (2016).
  - [3] M. I. Rabinovich, R. Huerta, and G. Laurent, *Science* **321**, 48 (2008).
  - [4] J. Britz, D. Van De Ville, and C. M. Michel, *NeuroImage* **52**, 1162 (2010).
  - [5] S. J. Kiebel, K. von Kriegstein, J. Daunizeau, and K. J. Friston, *PLoS Comput Biol* **5**,

- e1000464 (2009).
- [6] C. Bick and M. I. Rabinovich, *Phys Rev Lett* **103**, 218101 (2009).
  - [7] M. I. Rabinovich, A. N. Simmons, and P. Varona, *Trends Cogn Sci* **19**, 453 (2015).
  - [8] A. D. Horschler, K. A. Daltorio, H. J. Chiel, and R. D. Quinn, *Bioinspir Biomim* **10**, 026001 (2015).
  - [9] J. O’Keefe and J. Dostrovsky, *Brain Res* **34**, 171 (1971).
  - [10] D. H. Hubel and T. N. Wiesel, *J Physiol* **148**, 574 (1959).
  - [11] S.-i. Amari, *Biol Cybern* **27**, 77 (1977).
  - [12] Z. P. Kilpatrick, B. Ermentrout, and B. Doiron, *J Neurosci* **33**, 18999 (2013).
  - [13] M. Wildie and M. Shanahan, *Chaos* **22**, 043131 (2012).
  - [14] E. Tognoli and J. A. S. Kelso, *Neuron* **81**, 35 (2014).
  - [15] C. Bick and E. A. Martens, *New J Phys* **17**, 033030 (2015).
  - [16] M. Panaggio and D. M. Abrams, *Nonlinearity* **28**, R67 (2015).
  - [17] E. Schöll, *Eur Phys J-Spec Top* **225**, 891 (2016).
  - [18] D. Pazó and E. Montbrió, *Phys Rev X* **4**, 011009 (2014).
  - [19] C. R. Laing, *Phys Rev E* **90**, 010901 (2014).
  - [20] Chimeras on a finite ring of oscillators are subject to a pseudo-random, undirected drift unless the symmetry of the ring is broken [15].
  - [21] P. Ashwin and O. Burylko, *Chaos* **25**, 013106 (2015).
  - [22] C. Bick and P. Ashwin, *Nonlinearity* **29**, 1468 (2016).
  - [23] C. Bick, *J Nonlinear Sci* **27**, 605 (2017).
  - [24] M. Rosenblum and A. Pikovsky, *Phys Rev Lett* **98**, 064101 (2007).
  - [25] C. Bick, P. Ashwin, and A. Rodrigues, *Chaos* **26**, 094814 (2016).
  - [26] J. Acebrón, L. Bonilla, C. Pérez Vicente, F. Ritort, and R. Spigler, *Rev Mod Phys* **77**, 137 (2005).
  - [27] P. Ashwin and A. Rodrigues, *Physica D* **325**, 14 (2016).
  - [28] T. Nowotny and M. I. Rabinovich, *Phys Rev Lett* **98**, 1 (2007).
  - [29] M. A. Komarov, G. V. Osipov, and C. S. Zhou, *Phys Rev E* **87**, 022909 (2013).
  - [30] C. Bick, M. Sebek, and I. Z. Kiss, “Engineering Weak Chimeras in Chemical Oscillator Networks,” (2017), in prep.
  - [31] E. A. Martens, *Phys Rev E* **82**, 016216 (2010).

- [32] P. Ashwin and J. W. Swift, J Nonlinear Sci **2**, 69 (1992).
- [33] M. Golubitsky and I. Stewart, *The Symmetry Perspective*, Progress in Mathematics, Vol. 200 (Birkhäuser Verlag, Basel, 2002) pp. xviii+325pp.
- [34] C. Bick and et al, “Heteroclinic Networks of Weak Chimeras,” (2017), in prep.
- [35] By evaluating the saddle values we can show that  $\varepsilon < -r$  implies that the heteroclinic cycle is attracting [34].
- [36] B. Ermentrout, *Simulating, Analyzing, and Animating Dynamical Systems: A Guide to XPPAUT for Researchers and Students* (Society for Industrial and Applied Mathematics, 2002).
- [37] Except for some set of initial conditions of zero Lebesgue measure.
- [38] V. Kirk and M. Silber, Nonlinearity **7**, 1605 (1994).
- [39] O. Burylko and A. Pikovsky, Physica D **240**, 1352 (2011).
- [40] J. Sieber, O. E. Omel’chenko, and M. Wolfrum, Phys Rev Lett **112**, 054102 (2014).
- [41] M. Komarov and A. Pikovsky, Phys Rev E **84**, 016210 (2011).
- [42] P. Ashwin and C. Postlethwaite, Physica D **265**, 26 (2013).
- [43] M. J. Field, J Nonlinear Sci **25**, 779 (2015).
- [44] S. Castro and A. Lohse, SIAM J Appl Dyn Syst **15**, 1085 (2016).
- [45] H. Kori, C. G. Rusin, I. Z. Kiss, and J. L. Hudson, Chaos **18**, 026111 (2008).